Fully-coupled model for the direct and inverse effects in cubic magnetostrictive materials

Phillip G. Evans, Marcelo J. Dapino

The Ohio State University, 201 W 19th Ave, Columbus, OH 43210 USA

ABSTRACT

A fully-coupled, nonlinear model is presented that characterizes the 3-D strain and magnetization response of magnetostrictive materials to magnetic fields and mechanical stresses. The model provides an efficient framework for characterization, design, and control of Galfenol ($Fe_{1-x}Ga_x$) devices with 3-D functionality subjected to combined magnetic field and stress loading. A thermodynamic approach is taken to determine possible domain orientations considering the magnetocrystalline anisotropy, magnetomechanical, and Zeeman energies. The domain configuration is determined through minimization of the total Gibbs energy of a collection of domains. To incorporate material texture, the orientation of the applied field and stress with respect to the local crystal orientation is included as a statistically distributed parameter. Hysteresis due to irreversible domain wall motion is modeled by accounting for the energy loss due to domain wall pinning sites.

Keywords: Galfenol, magnetization, magnetostriction, model, 3-D, hysteresis, polycrystallinity

1. INTRODUCTION

With the advent of magnetostrictive Galfenol which has steel-like structural properties, models that predict Galfenols 3-D magnetomechanical behavior have become increasingly important. Magnetic anisotropy and material texture cause the magnetization and strain response to magnetic fields and stresses to depend heavily on the application direction. Magnetostrictive devices have often been limited to unidirectional loading, due in part to the brittleness of Terfenol-D. Accurate, nonlinear, and low-order transducer models[1] have typically relied on 1-D constitutive models such as Jiles' Theory of Ferromagnetic Hysteresis,[2] the Preisach model, and Smith's homogenized energy framework.[3] This paper describes a low-order constitutive model for 3-D magnetomechanical coupling which, owing to its computational efficiency, is ideal for design and control of general Galfenol transducers.

Recently, Datta, Atulasimha, and Flatau[4] presented a 3-D, quasi-static transducer model for single-crystal Galfenol in bending which couples Euler-Bernoulli beam theory with the Armstrong model[5] for characterizing magnetomechanical behavior. The 3-D Armstrong model has also been used to model the magnetomechanical behavior of polycrystals[6] and hysteresis of single crystals.[7] The Armstrong model is an anhysteretic statistical model which assumes that magnetic domain orientations (ϕ, θ) follow a Boltzmann distribution. Magnetomechanical coupling is incorporated through a stress-induced anisotropy term in the total energy (E) used in the distribution. In the Armstrong model, a bulk quantity is calculated by an energy weighted integral of the point-wise quantity over all possible domain orientations,

$$\bar{Q} = \frac{\int_0^{\pi}\int_0^{2\pi} Q(\phi,\theta)e^{-E(\phi,\theta)/\Omega}d\theta d\phi}{\int_0^{\pi}\int_0^{2\pi} e^{-E(\phi,\theta)/\Omega}d\theta d\phi}. \tag{1}$$

The double integral serves to smooth the sharp transitions predicted by directed minimization of the total energy. Since the energy terms in the Armstrong model depend only on magnetization orientation, it is only accurate for single crystals when domain rotation is the dominant magnetization process, i.e., collinear field and stress applications with moderate compressive stress.

Further author information: (Send correspondence to M.J.D.)
M.J.D.: E-mail: dapino.1@osu.edu, Telephone: 1-614-688-3689
P.G.E.: E-mail: evans.895@osu.edu, Telephone: 1-614-247-7480

Behavior and Mechanics of Multifunctional and Composite Materials 2008,
edited by Marcelo J. Dapino, Zoubeida Ounaies, Proc. of SPIE Vol. 6929, 692922, (2008)
0277-786X/08/$18 · doi: 10.1117/12.776558

To characterize, design, and control general Galfenol devices with 3-D functionality it is necessary to quantify the effects of domain wall motion, material texture, hysteresis, and transducer geometry. Extending the rotational model (1) to include these effects comes at great computational expense, hence limiting the utility of the resulting model. For example, to include irreversible domain wall motion (reversible domain wall motion is neglected) Atulasimha and Akrhas[7] approximate the double integral in (1) with a summation of 98 point evaluations, which leads to 98 ordinary differential equations to be solved. Armstrong's approach to including irreversible domain wall motion is less demanding as it only considers 8 domain orientations corresponding to the 8 easy crystal directions.[8] However, it is accurate only when the applied field or stress is aligned with an easy crystal axis. Extending (1) to include texture effects (neglecting grain boundary interactions) requires a summation of double integrals.[6]

To solve the boundary-value problem of general Galfenol transducers it is necessary to couple Maxwell's equations with strain-displacement and force-equilibrium equations through a constitutive model relating magnetization and strain to stress and magnetic field. This system of partial differential equations must be discretized for numerical solution and the constitutive model must be evaluated at each node. A computationally efficient constitutive model is thus highly desirable. In this paper we present a 3-D (in tensorial sense) constitutive model derived from thermodynamic principles which describes magnetization and strain as a function of applied magnetic field and stress. In this model, smooth behavior is achieved without the need of a double integral such as (1) thus making the model both accurate and numerically efficient.

2. CONSTITUTIVE MODEL

Ferromagnetic materials below the Curie temperature have regions of uniform magnetization M_s where the atomic magnetic moments are aligned with each other. These regions of uniform magnetization are called magnetic domains. Magnetic domains have preferred orientations which depend on the magnetic anisotropy and on the applied magnetic field and stress. These orientations are preferred because they attain thermodynamic equilibrium. For a given magnetic field and stress, multiple preferred or equilibrium orientations may exist. In the absence of magnetic field and stress, Galfenol has six equilibrium orientations in the $\langle 100 \rangle$ directions and Terfenol-D ($Tb_{0.3}Dy_{0.7}Fe_{1.9}$) has eight in the $\langle 111 \rangle$ directions. As magnetic fields and stresses are applied, the equilibrium orientations rotate towards the field direction and perpendicular to the stress direction. When magnetic domains rotate, the magnetomechanical coupling causes a lattice strain termed magnetostriction. The total magnetization and magnetostriction are the vector sum of the domain magnetization and magnetostriction, respectively. When thermodynamic equilibrium is achieved, the total magnetization $\bar{\mathbf{M}}$ and magnetostriction $\bar{\mathbf{S}}$ of a material having r equilibrium domain orientations $\hat{\mathbf{m}}^k$ are the sum of the magnetization $M_s\hat{\mathbf{m}}^k$ and magnetostriction $\hat{\mathbf{S}}^k$ due to each equilibrium orientation, weighted by the volume fraction $\hat{\xi}^k$ of domains in each orientation

$$\bar{\mathbf{M}} = M_s \sum_{k=1}^{r} \hat{\xi}^k \hat{\mathbf{m}}^k, \qquad \bar{\mathbf{S}} = \sum_{k=1}^{r} \hat{\xi}^k \hat{\mathbf{S}}^k. \tag{2}$$

The equilibrium domain orientations and magnetostrictions are found from the Gibbs energy of a single domain and the equilibrium domain volume fractions are found from the Gibbs energy of a collection of domains.

2.1. Equilibrium Domain Orientations

The internal energy of a magnetic domain with orientation $\mathbf{m} = [m_1 \quad m_2 \quad m_3]$ is due to the magnetocrystalline anisotropy energy, which can be expressed as a series expansion. After considering the cubic crystal symmetry and neglecting higher order terms, the expression for cubic materials is[9]

$$U(\mathbf{m}) = K_4 \left(m_1 m_2 + m_2 m_3 + m_3 m_1 \right), \tag{3}$$

where K_4 is the fourth-order, cubic anisotropy constant. The Gibbs free energy is

$$G(\mathbf{H}, \mathbf{T}) = U(\mathbf{m}) - \mathbf{S} \cdot \mathbf{T} - \mu_0 M_s \mathbf{m} \cdot \mathbf{H}, \tag{4}$$

where $\mathbf{T}$ is the six-element stress vector with the first three components the longitudinal stresses and the last three the shear stresses. Parameter $\mathbf{H}$ is the magnetic field and $\mathbf{S} = \mathbf{S}(\mathbf{m})$ is the magnetostriction with longitudinal components[9]

$$S_i = -\frac{3}{2}\lambda_{100} m_i^2, \quad i = 1, 2, 3 \tag{5}$$

and shear components

$$\begin{aligned} S_4 &= -3\lambda_{111} m_1 m_2, \\ S_5 &= -3\lambda_{111} m_2 m_3, \\ S_6 &= -3\lambda_{111} m_3 m_1. \end{aligned} \tag{6}$$

These expressions are derived by balancing the magnetic anisotropy, elastic, and magnetoelastic coupling energies.[9]

For $K_4 > 0$, the internal energy has six minima or easy axes ($r = 6$) in the $\langle 100 \rangle$ directions and for $K_4 < 0$, the internal energy has eight minima or easy axes ($r = 8$) in the $\langle 111 \rangle$ directions. Applied magnetic and magnetomechanical work rotates domains away from the easy axes towards the magnetic field direction and perpendicular to the longitudinal stress direction (see Figure 1). The equilibrium domain orientations $(\hat{\mathbf{m}}^k; k = 1, ..., r)$, needed for calculation of the bulk magnetization (2), are obtained through the conditions $\partial G / \partial m_i = 0$ with the constraint $m_1^2 + m_2^2 + m_3^2 = 1$. The equilibrium magnetostrictions $(\hat{\mathbf{S}}^k; k = 1, ..., r)$, needed for calculation of the bulk magnetostriction (2), are obtained by evaluating relations (5) and (6) using the equilibrium domain orientations, $\hat{\mathbf{S}}^k = \mathbf{S}(\hat{\mathbf{m}}^k)$.

2.2. Equilibrium Domain Volume Fractions

The bulk magnetization and magnetostriction due to a collection of domains is the sum of the products of the magnetization and magnetostriction equilibria with the respective volume fraction of domains ξ^k in the k^{th} equilibrium (see equation 2).

If the sample geometry is known, the domain volume fractions can be determined from minimization of the magnetostatic energy where the demagnetizing field can be calculated from approximate geometry factors or through the finite element method. For an unspecified geometry with homogeneous stress and field, the domain volume fractions can be determined by minimizing a total Gibbs energy potential which includes the entropy of a collection of domains. The entropy of a system of N units (in this case domains) with r possible energy states has been given by terHaar[10]

$$\eta = \frac{k_B}{NV} \ln \left(\frac{N!}{N_1! N_2! N_3! ... ! N_r!} \right), \tag{7}$$

where N_k is the number domains in the k^{th} energy state, N is the total number of domains, V is the control volume and k_B is Boltzmann's constant. Using Stirling's approximation and substituting $\xi_k = N_k / N$, the entropy is

$$\eta = -\frac{k_B}{V} \sum_{k=1}^{r} \xi^k \ln \xi^k. \tag{8}$$

The total Gibbs energy is then given by

$$\bar{G} = -\eta\theta + \sum_{k=1}^{r} \xi^k G^k, \tag{9}$$

where θ is temperature and $G^k(\mathbf{H}, \mathbf{T}) = U(\hat{\mathbf{m}}^k) - \hat{\mathbf{S}}^k \cdot \mathbf{T} - \mu_0 M_s \hat{\mathbf{m}}^k \cdot \mathbf{H}$. The equilibrium domain configuration $\hat{\xi}_k$ is obtained from the equilibrium conditions $\partial \bar{G} / \partial \xi_k = 0$, constrained to $\sum_{k=1}^{r} \xi^k = 1$, which yields

$$\hat{\xi}^k = \frac{e^{-G^k V / k_B \theta}}{\sum_{j=1}^{r} e^{-G^j V / k_B \theta}}. \tag{10}$$

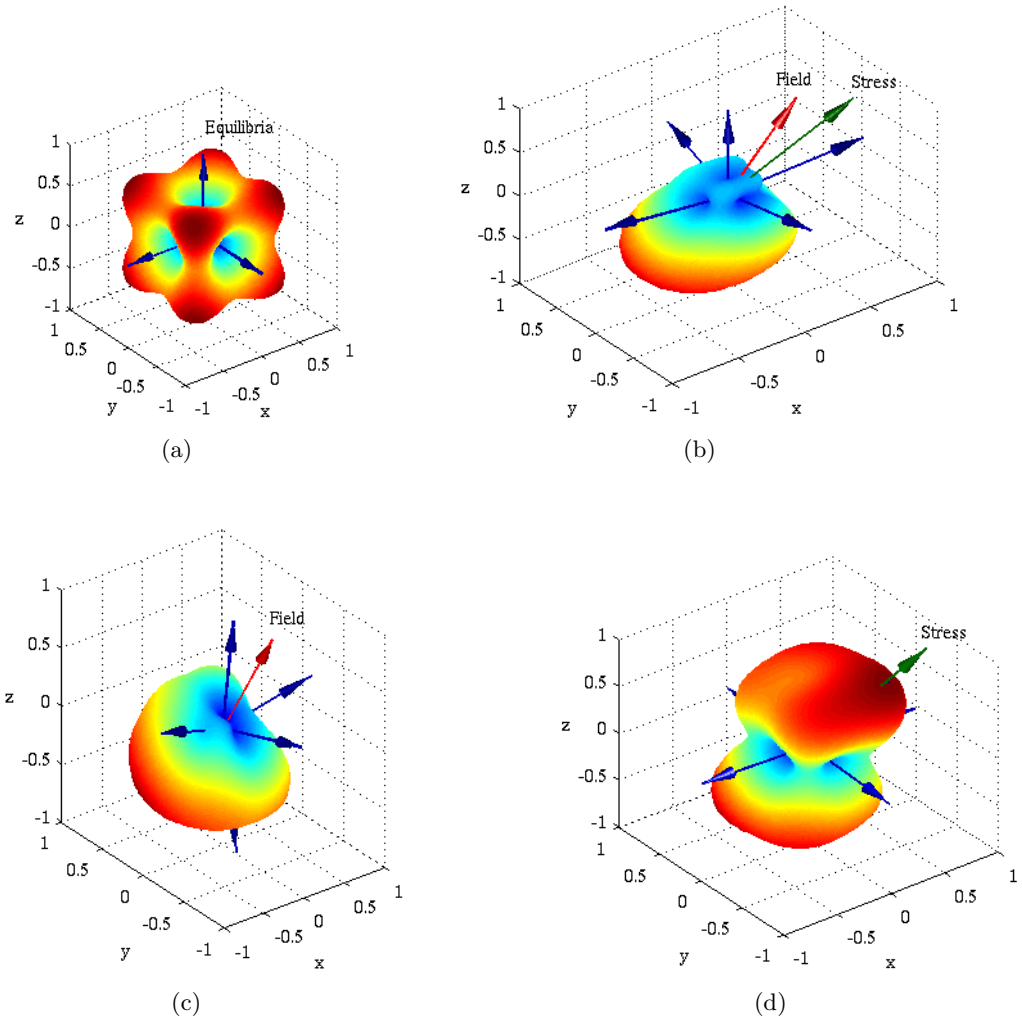

Figure 1. Gibbs energy equilibrium orientations with (a) no field or stress (b) field and stress (c) field only (d) stress only.

Substituting (10) into (2) gives the bulk magnetization and magnetostrain

$$\bar{\mathbf{M}} = \frac{\sum_{k=1}^{r} M_s \hat{\mathbf{m}}^k e^{-G^k V/k_B\theta}}{\sum_{k=1}^{r} e^{-G^k V/k_B\theta}}, \qquad \bar{\mathbf{S}} = \frac{\sum_{k=1}^{r} \hat{\mathbf{S}}^k e^{-G^k V/k_B\theta}}{\sum_{k=1}^{r} e^{-G^k V/k_B\theta}}. \tag{11}$$

Relations (11) are similar to (1) when $\Omega = k_B\theta/V$, $G = E$ and the integrals are discretized. However, they differ in that (11) was derived through thermodynamic principles and is more computationally efficient as it involves a summation of only six terms whereas (1) requires hundreds of summations depending on the numerical integration algorithm and desired accuracy. Simulation of the inverse effect in the [100] and [110] directions is shown in Figure 2 and the direct effect in Figure 3. It is noted that smooth constitutive behavior has been achieved without integration. Figure 2(d) shows a decrease in magnetostriction at high fields because domains rotate away from the the [100] crystal direction, the maximum magnetostriction direction, towards the [110] direction which is near the [111] minimum magnetostriction direction and may even have negative magnetostriction depending on the Gallium content.

2.3. Polycrystallinity

Polycrystallinity is incorporated by considering non-interacting regions of defect-free crystal lattice having a statistically distributed orientation with respect to the coordinate frame of the applied field and stress. This approach is similar to that of Appino, Valsania, and Basso[11] which considers in-plane domain rotations in polycrystalline materials with uniaxial anisotropy. The bulk magnetization takes the form

$$\bar{\mathbf{M}}_{poly} = \int_0^{2\pi} \int_0^{\pi} \bar{\mathbf{M}}(\mathbf{H}, \mathbf{T}, \phi_0, \theta_0)\nu(\phi_0, \theta_0) d\phi_0 d\theta_0, \tag{12}$$

where (ϕ_0, θ_0) is the orientation, in spherical coordinates, of the field and stress with respect to the crystal lattice. The grain orientation distribution ν depends on the material texture, which influences the bulk magnetostriction.[12] Consider for example cylindrical rods grown by the techniques described by Summers et al. [13]. Orientation imaging microscropy shows a high degree of grain alignment with grains narrowly distributed about the rod axis. An appropriate distribution when the field and stress are applied along the rod axis would be Gaussian in ϕ_0 and uniform in θ_0

$$\nu(\phi_0, \theta_0) = \frac{e^{-\phi_0^2/2\sigma^2}}{\sigma\sqrt{2\pi}} \frac{e^{-\theta_0^2/2\sigma^2}}{\sigma\sqrt{2\pi}}, \tag{13}$$

where σ is the standard deviation of the grain misalignment angle. Since the $\langle 100 \rangle$ direction has the largest magnetostriction, any off-axis grains tend to decrease the bulk magnetostriction,[13] hence as the distribution broadens (increasing σ), the maximum magnetostriction decreases (see Figure 4.)

2.4. Hysteresis

Armstrong[8] incorporated irreversible domain wall motion in a rotational model by including losses due to uniformly distributed pinning sites in the evolution of the domain volume fractions. We take a similar approach,

$$\frac{d\xi}{dH} = (\xi_{\text{an}} - \xi)/k, \tag{14}$$

where k is proportional to the pinning site energy and ξ_{an} is the anhysteretic domain volume fraction given by (10). This implementation differs from that of Armstrong in that the domains are allowed to rotate in order to minimize the Gibbs energy whereas Armstrong only considered the 8 fixed $\langle 111 \rangle$ orientations which correspond to the easy crystal axes or internal energy minima in Terfenol-D. Neglecting domain rotation limits the accuracy of the model, especially when operated in directions away from the easy axes. Atulasimha and Akrhas[7] improved the accuracy by considering 98 fixed orientations corresponding to important orientations with regards to the internal energy (magnetocrystalline anisotropy energy). Allowing domains to rotate in order to minimize the Gibbs energy is thermodynamically consistent and reduces the number of domain orientations to be tracked to 6 while preserving accuracy.

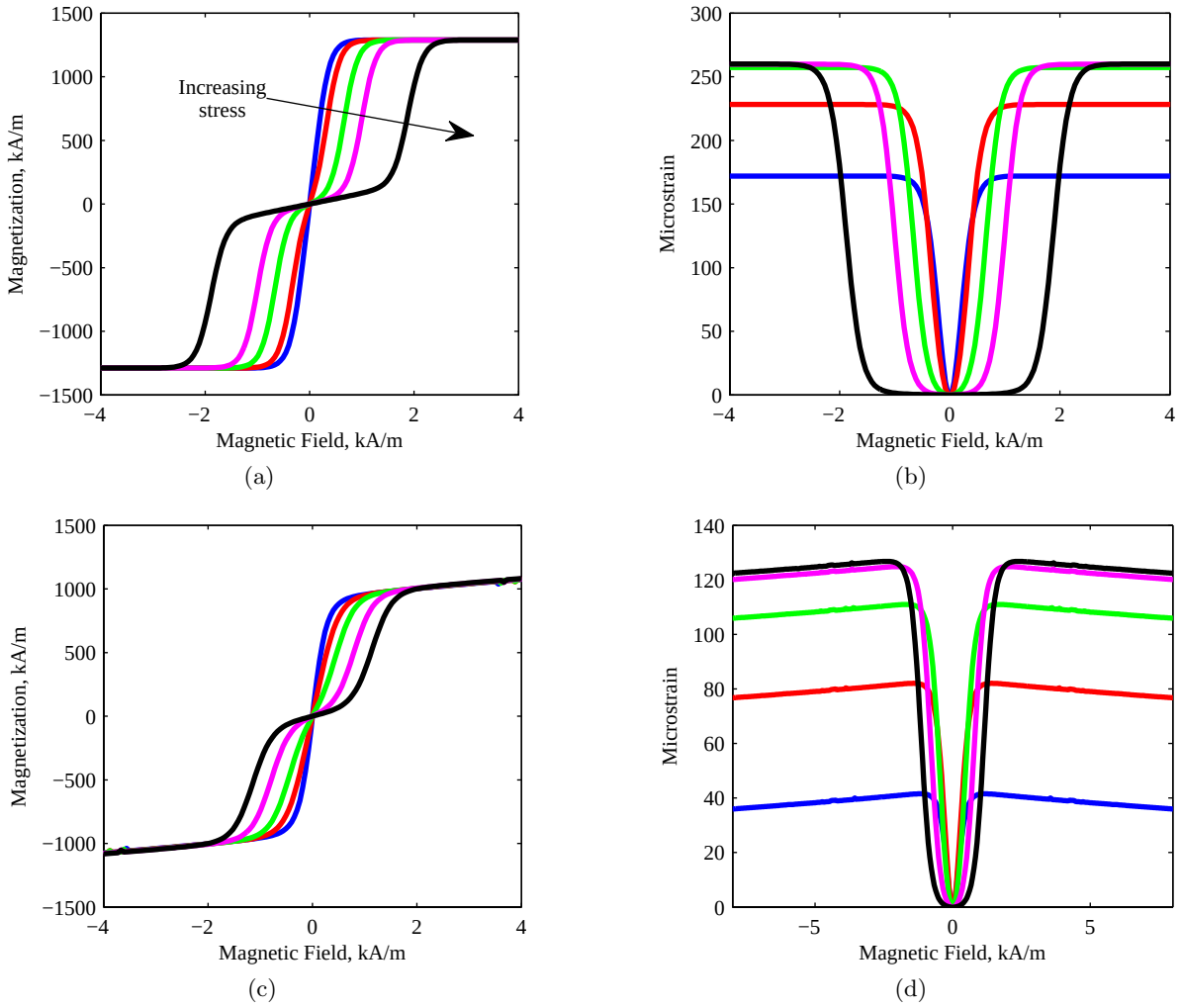

Figure 2. Simulation of the inverse effect at various stress levels for the (a),(b) [100] direction and (c),(d) [110] direction.

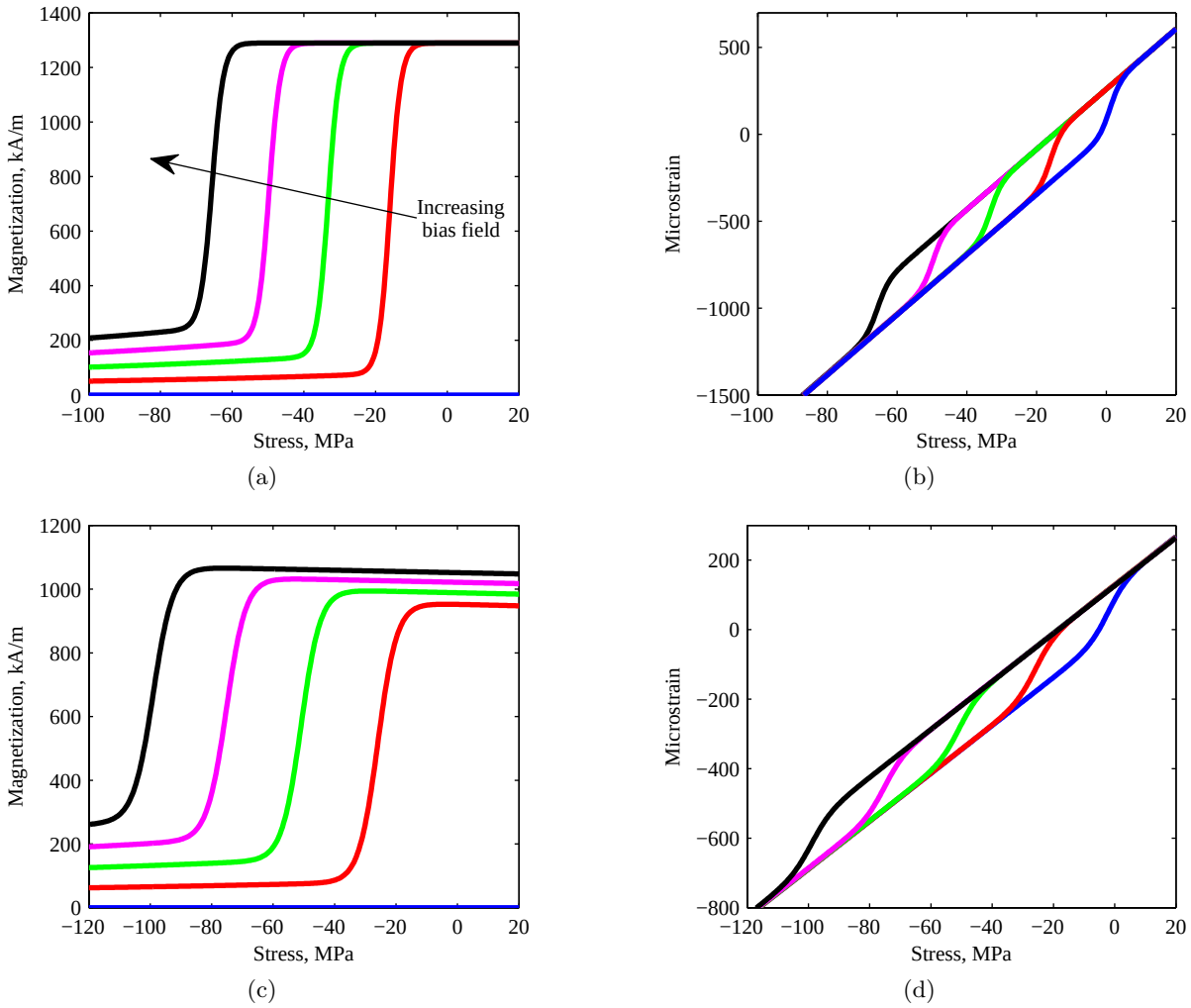

Figure 3. Simulation of the direct effect at various stress levels for the (a),(b) [100] direction and (c),(d) [110] direction.

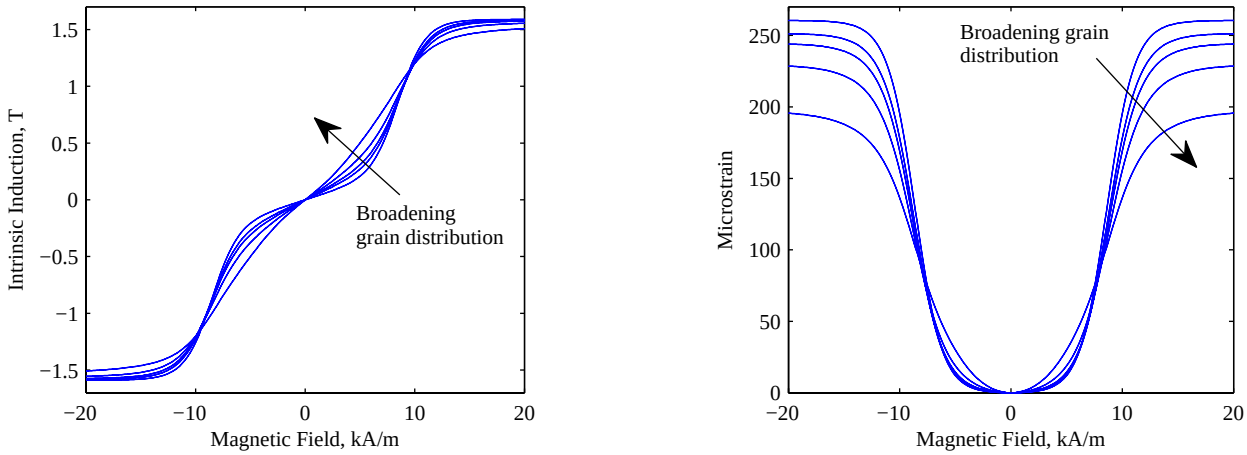

Figure 4. Inverse effect simulation using (12) and (13) with increasing grain misalignment.

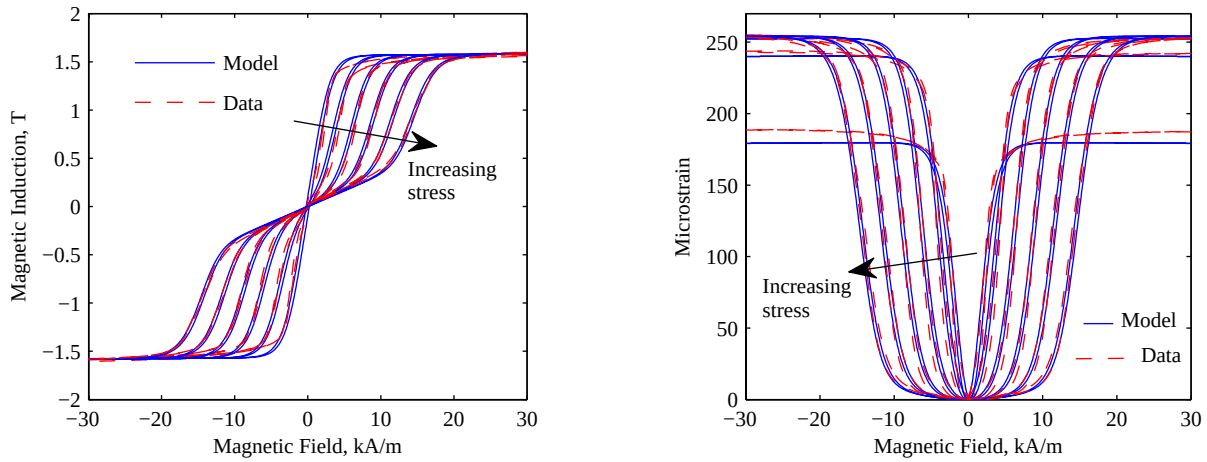

Figure 5. Comparison of Galfenol inverse effect data with the hysteretic, polycrystalline model at stress levels of $-1.38, -13.8, -41.4, -55.2, -69$ MPa.

3. EXPERIMENTAL VALIDATION

The polycrystal formulations (12) and (13) and hysteresis model (14) were used to describe the magnetization and strain response to magnetic field at 6 levels of constant compressive stress. The integral (12) was computed numerically with a 4 point Gauss-Quadrature integration. The sample is research grade $Fe_{81.6}Ga_{18.4}$ from Etrema Products Inc., produced with an advanced Bridgeman method which results in a polycrystalline rod with a large percentage of the grains having the [100] direction oriented along the axis of the rod. Magnetic field and induction were measured along the rod axis. The model parameters were determined through a least-squares algorithm with initial values in the parameter optimization algorithm chosen to be consistent with the literature. The optimized parameters were $k = 300$ A/m, $\sigma = 7.10$ deg, $M_s = 1.26 \times 10^{-3}$ kA/m, $K_4 = 36.0$ kJ/m^3, $\lambda_{100} = 174$ $\mu\epsilon$, $\lambda_{111} = -13.3$ $\mu\epsilon$, and $k_B\theta/V = 1.6$ kJ/m^3. The accuracy of the model is illustrated by the fact that the model parameters were optimized for only one data set while the simulations agree well with all the data sets. While the error was small for all data sets, the error is larger for the low-stress data sets where domain wall motion is more prevalent. This may be attributed to the absence of reversible domain wall motion in the model.

4. CONCLUDING REMARKS

A low-order, 3-D constitutive model relating magnetization and strain to magnetic field and stress has been developed through thermodynamic principles. By including entropy in the Gibbs energy, the basic model framework achieves smooth constitutive behavior without integration. As a result, the framework is extended to include irreversible domain wall motion and material texture without making it too cumbersome for use in distributed parameter, general transducer models which are often solved with the finite-element method, requiring evaluation of the material constitutive model at each node. Comparison of the model to experiment has shown it to accurately model the magnetization and strain response over a broad range of magnetic fields and stresses. The efficiency and accuracy of the model makes it ideal for lumped parameter transducer models which may be used for model-based, real-time control of magnetostrictive devices. While accurate, low-order transducer models have been developed for magnetostrictive devices operated in 1-D modes, the framework developed here can be used for characterization, design, and control of Galfenol devices capable of 3-D magnetic field and stress loading.

ACKNOWLEDGMENTS

We wish to acknowledge the financial support by the Office of Naval Research, MURI grant #N000140610530.

REFERENCES

1. M. J. Dapino, R. C. Smith, and A. B. Flatau, "Structural magnetic strain model for magnetostrictive transducers," *IEEE Transactions on Magnetics* **36**, pp. 545–556, May 2000.
2. X. Tan and J. S. Baras, "Modeling and control of hysteresis in magnetostrictive actuators," *Automatica* **40**(9), pp. 1469–1480, 2004.
3. W. S. Oates, P. G. Evans, R. C. Smith, and M. J. Dapino, "Experimental implementation of a hybrid nonlinear control design for magnetostrictive actuators," *Journal of Dynamic Systems, Measurement, and Control* . In review.
4. S. Datta, J. Atulasimha, and A. B. Flatau, "Modeling of magnetostrictive galfenol sensor and validation using four point bending test," *Journal of Applied Physics* **101**, 2007.
5. W. D. Armstrong, "Magnetization and magnetostriction processes," *Journal of Applied Physics* **81**(5), pp. 23217–2326, 1997.
6. J. Atulasimha, A. B. Flatau, and E. Summers, "Characterization and energy-based model of the magnetomechanical behavior of polycrystalline iron–gallium alloys," *Smart Materials and Structures* **16**, pp. 1265–1276, 2007.
7. J. Atulasimha and G. Akhras, "Comprehensive 3-D hysteretic magnetomechanical model and its validation with experimental ⟨110⟩ singe-crystal iron-gallium behavior," *To be published* , 2007.
8. W. D. Armstrong, "An incremental theory of magneto-elastic hysteresis in pseudo-cubic ferromagnetostrictive alloys," *Journal of Magnetism and Magnetic Materials* **263**, p. 208, 2003.
9. C. Kittel, "Physical theory of ferromagnetic domains," *Review of Modern Physics* **21**, pp. 541–583, Oct 1949.
10. D. ter Haar, *Elements of Statistical Mechanics*, p. 158. Butterworth-Heinemann, 3rd ed., 1995.
11. C. Appino, M. Valsania, and V. Basso, "A vector hysteresis model including domain wall motion and coherent rotation," *Physica B* **275**(1-3), pp. 103–106, 2000.
12. R. A. Kellogg, A. Flatau, A. E. Clark, M. Wun-Fogle, and T. Lograsso, "Quasi-static transduction characterization of Galfenol," *Journal of Intelligent Material Systems and Structures* **16**, pp. 471–479, 2005.
13. E. Summers, T. A. Lograsso, J. D. Snodgrass, and J. Slaughter, "Magnetic and mechanical properties of polycrystalline Galfenol," in *Proc. of SPIE*, D. C. Lagoudas, ed., *Smart Structures and Materials 2004: Active Materials: Behavior and Mechanics* **5387**, pp. 448–459, 2004.